

Axion detection through resonant photon-photon collisions

K. A. Beyer,^{1,*} G. Marocco,^{1,†} R. Bingham,^{2,3} and G. Gregori¹

¹*Department of Physics, University of Oxford, Parks Road, Oxford OX1 3PU, UK*

²*Rutherford Appleton Laboratory, Chilton, Didcot OX11 0QX, UK*

³*Department of Physics, University of Strathclyde, Glasgow G4 0NG, UK*

We investigate the prospect of an alternative laboratory-based search for the coupling of axions and axion-like particles to photons. Here, the collision of two laser beams resonantly produces axions, and a signal photon is detected after magnetic reconversion, as in light-shining-through-walls (LSW) experiments. Conventional searches, such as LSW or anomalous birefringence measurements, are most sensitive to axion masses for which substantial coherence can be achieved; this is usually well below optical energies. We find that using currently available high-power laser facilities, the bounds that can be achieved by our approach outperform traditional LSW at axion masses between 0.5 – 6 eV, set by the optical laser frequencies and collision angle. These bounds can be further improved through coherent scattering off laser substructures, probing axion-photon couplings down to $g_{a\gamma\gamma} \sim 10^{-8} \text{ GeV}^{-1}$, comparable with existing CAST bounds.

The Standard Model of particle physics allows for charge-parity (CP) violation in the electroweak and strong sectors. While the former is experimentally established, the latter is constrained by neutron electromagnetic dipole measurements to be negligibly small, with no natural explanation. This is the strong CP problem. One of the most well-motivated solutions to this problem is the axion proposal by Peccei and Quinn [1, 2]. With the addition of a chiral $U(1)_{\text{PQ}}$ symmetry, the CP-violating parameter is dynamically driven to zero. It has been subsequently noted that the pseudo-Goldstone bosons arising from the spontaneous breaking of $U(1)_{\text{PQ}}$, the QCD axion, can make up a substantial fraction or the entirety of the dark matter abundance [3, 4], and perhaps also be responsible for the initial magnetisation of the Universe [5]. Similar pseudoscalars, known as axion-like particles (ALPs), readily arise in the low-energy spectrum of string theory [6, 7]. A number of experiments aiming at the discovery of axions have already placed bounds [8] on the available parameter space, with varying degrees of model-dependence; we use the term axion to refer to both the QCD axion and CP-conserving ALPs.

An axion couples to Standard Model photons via

$$\mathcal{L}_p = -\frac{1}{4}F^{\mu\nu}F_{\mu\nu} + \frac{1}{2}(\partial_\mu a)(\partial^\mu a) - \frac{1}{2}m_a^2a^2 + \frac{1}{4}g_{a\gamma\gamma}a\tilde{F}^{\mu\nu}F_{\mu\nu} \quad (1)$$

with a the axion field, m_a the axion mass, F the electromagnetic field-strength tensor and $\tilde{F}^{\mu\nu} = \frac{1}{2}\epsilon^{\mu\nu\sigma\rho}F_{\sigma\rho}$ its dual. We will be interested in constraining the axion-photon coupling $g_{a\gamma\gamma}$. When interested in a CP-conserving scalar field s , the interaction term is instead

$$\mathcal{L}_s \supset \frac{1}{4}g_{s\gamma\gamma}sF^{\mu\nu}F_{\mu\nu}. \quad (2)$$

The axion-photon coupling term gives rise to a cubic interaction of an axion with two photons, and can be expressed as $g_{a\gamma\gamma}a\mathbf{E} \cdot \mathbf{B}$ for pseudoscalars or $g_{a\gamma\gamma}a(E^2 - B^2)$ for scalars. In the presence of an external magnetic

field this leads to axion-photon mass mixing [9, 10], and implies a range of signatures which can, in principle, be measured in a laboratory-based experiment.

The most stringent bounds on $g_{a\gamma\gamma}$ apply to axion masses below 1 meV. In the higher mass region around 1 eV the strongest bounds, excluding purely astrophysical arguments derived from stellar cooling times, are placed by the CAST experiment [11], a helioscope sensitive to the axion flux produced by the Primakoff effect [12] in the Sun. Above 1 eV, constraints from Primakoff coherent solar axion to photon conversion in crystals place stronger constraints [13]. Due to the astrophysical origin of the axions and the consequential lack of control over the production, the possibility of model dependence must be seriously taken into account. Environmental conditions in the Sun such as high photon energy and non-zero plasma frequency affect the axion-photon effective coupling [14]. Similar arguments can also apply to constraints derived from stellar cooling, with further ambiguities introduced by stellar cooling models. As such, we focus on complementary, model-independent bounds given by purely terrestrial experiments.

Currently running searches like the OSQAR [15] experiment implement a Sikivie-style LSW scheme [9] to detect the mass mixing. A laser beam propagating in a magnetic field can spontaneously create axions, which, being weakly coupled, pass through an intervening wall. Behind the wall, any axions entering the reconversion magnetic field may mix back into photons and be detected. This mass mixing is enhanced if the magnetic field contains momentum modes corresponding to the momentum exchange between the axion and the photon. As such, the large momentum exchange needed for conversion of non-relativistic axions suppresses the rate as the modes are set by the inverse length of the external magnetic field region.

Other laboratory axion searches include the PVLAS collaboration [16], with the goal of looking at induced birefringence as a polarised laser beam traverses a mag-

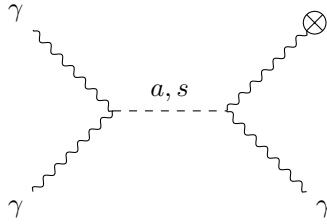


FIG. 1. The Feynman diagram for the conversion of two photons into an axion, which decays into a photon in an external magnetic field.

netic field region. The change in polarisation receives contributions from both QED [17] and axion [10] interactions. The leading QED contribution is a four-vertex, one-loop process, which competes against the tree-level axion contribution. The exclusion bounds of PVLAS are thus limited by the requirement that the latter process is the dominant one. Once axion interactions are smaller than the leading order Standard Model prediction, one must be careful of, for instance, hadronic contributions. Given the difficulty this presents in other precision measurements [18], disentangling each independent contribution becomes very challenging. PVLAS experiments are close to such a limit, suggesting new techniques are required to probe axion couplings below those bounds.

Our proposal aims to improve current laboratory searches by adopting an alternative axion-production mechanism. Here we propose to generate axions via the collision of two laser beams. Axions, being very light and weakly coupled, are well suited to experiments involving a large number of photons, rather than collider searches with large background signals of soft particles. Lasers are ideal for this pursuit, and we expect that the non-linear dependence on the number of photons will allow a better scaling compared to the linear dependence in traditional LSW experiments, as we will discuss further below. Further, the possibility of resonant production at optical masses in such a set-up allows smaller couplings to be probed than traditional LSW experiments. Using pulsed lasers instead of continuous beams allows for the rejection of most background by exploiting coincident timing. This minimal approach can achieve sensitivities comparable to PVLAS. With the implementation of spatial modes on the laser beam, coherent generation of axions can significantly improve our bounds on $g_{a\gamma\gamma}$ down to 10^{-8} GeV^{-1} . These are comparable to bounds placed by CAST in the relevant mass region, but without any additional assumptions on the solar plasma.

We consider two photons, each with energy ω_j ($j = 1, 2$), colliding at an angle θ_{12} , as depicted in Fig. 1 and 2. The two incoming momenta define the scattering plane. The polarisation vectors can be expanded in terms of two basis vectors: one lying in the scattering plane and one perpendicular to it; both basis vectors are perpendicular

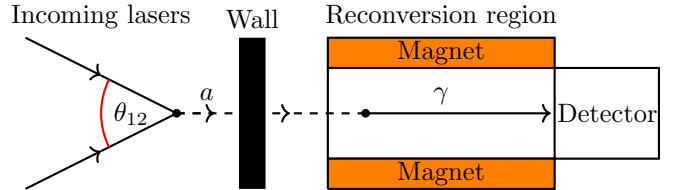


FIG. 2. A diagram of the experimental set-up. Photons from two lasers collide at in an interaction region, producing any hypothetical axions (either scalar or pseudoscalar). These pass through an intervening wall, and then reconvert into photons in the presence of a magnetic field. These photons are the signal detected.

to the momentum. The polarised matrix elements are

$$\mathcal{M}_{||,\perp}^p = -2g_{a\gamma\gamma}\omega_1\omega_2 \sin\left(\frac{\theta_{12}}{2}\right)^2, \\ \mathcal{M}_{||,||}^p = \mathcal{M}_{\perp,\perp}^p = 0,$$

where a subscript $||$ refers to in-plane and \perp to out-of-plane polarisation.

The corresponding cross-section is

$$\sigma = \frac{\pi}{4\omega_1\omega_2(\omega_1 + \omega_2)} \frac{|\mathcal{M}|^2}{\sqrt{2 - 2\cos\theta_{12}}} \delta(\omega_1 + \omega_2 - \omega_a) \quad (3)$$

where $\omega_a = \sqrt{m_a^2 + \omega_1^2 + \omega_2^2 + 2\omega_1\omega_2\cos\theta_{12}}$ is the axion energy and only $\mathcal{M} = \mathcal{M}_{||,\perp}^p$ contributes.

The appearance of a delta distribution is characteristic of energy-momentum conservation at a three point vertex. In a real experiment however the cross section is non-singular as the photons are provided by a laser beam of a finite pulse length τ , and additionally are drawn from a Gaussian distribution

$$f_j(\omega) = \frac{1}{\sqrt{2\pi\Delta_j^2}} \exp\left[-\frac{(\omega - \omega_j^0)^2}{2\Delta_j^2}\right] \quad (4)$$

with central frequency ω_j^0 and spectral width $\Delta_j \gtrsim \tau^{-1}$ dictated by the laser properties. Note also that in equation (3) we have implicitly taken the axion to be in an asymptotic state. This is a reasonable approximation given that its lifetime against stimulated decay to a photon is $\tau_{a\gamma\gamma} = 64\pi/N_j g_{a\gamma\gamma}^2 m_a^3$ [19] with N_j photons in the interaction region, which is always much longer than the laser pulse-length, $\tau \simeq 230 \text{ eV}^{-1}$. We thus treat the axion resonance as a delta distribution to be integrated against the Gaussian (4).

We now define the scattering probability as

$$P_{\gamma\gamma \rightarrow p} = \frac{1}{V} \sqrt{2 - 2\cos\theta_{12}} \int_0^\tau \sigma dt, \quad (5)$$

where V is the interaction volume of the two lasers. The angular dependence describes the flux of one beam

through the other. Given the probability for pseudoscalar production (5), the total number of incoherently produced axions is

$$N_p = N_1 N_2 P_{\gamma\gamma \rightarrow p}, \quad (6)$$

where N_j is the total number of photons of beam j in the interaction region.

Our proposed scheme for axion production can also be applied to scalars with a coupling given by equation (2). The associated matrix elements are

$$\begin{aligned} \mathcal{M}_{||,||}^s &= -2g_{s\gamma\gamma}\omega_1\omega_2 \sin\left(\frac{\theta_{12}}{2}\right)^2 \cos\theta_{12}, \\ \mathcal{M}_{\perp,\perp}^s &= -2g_{s\gamma\gamma}\omega_1\omega_2 \sin\left(\frac{\theta_{12}}{2}\right)^2, \\ \mathcal{M}_{||,\perp}^s &= 0. \end{aligned} \quad (7)$$

Note that scalars and pseudoscalar couple with opposite photon polarizations, making it possible to separate the two signatures independently. This is challenging to realise with other laser-based searches. The photon to scalar conversion probability is completely analogous to equation (5), with $p \rightarrow s$.

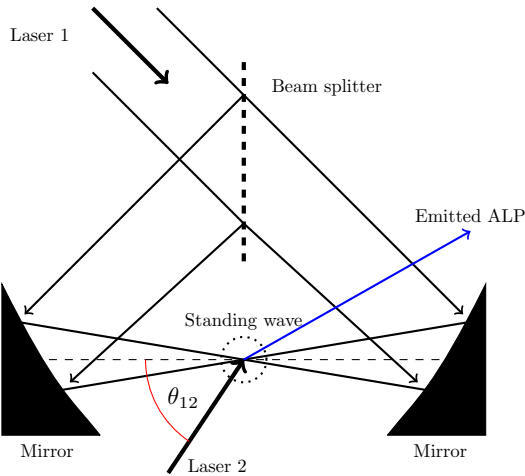


FIG. 3. A standing wave is formed in the circled region by passing a single laser pulse through a 50-50 beam splitter, each part of which then reflects off an off-axis parabolic mirror, as outlined in [20].

The probability of generating axions can be further enhanced by implementing spatial structure in one of the beams. In our proposed scheme, coherence must be achieved for large momentum transfer q , since axions become more non-relativistic as their mass approaches the photon frequency. In this case, a traditional LSW experiment suffers from interference effects which destroy coherence along the length ℓ of the interaction region when $q\ell \gtrsim 1$. This is avoided for the interaction of the probe beam with a standing wave, which can lead to a scattering amplitude somewhat similar to Bragg diffraction off of a

light grating [21]. In this case, a probe laser interacts with a standing wave produced by the other beam as shown in Fig. 3 (see also Ref. [20]). The standing wave is realised by reflecting a split laser beam off two off-axis mirrors such that they are counter-propagating at a common focus. Scattering is then coherent within any single half-period of the standing wave, leading to an overall cubic scaling with photon number (see below).

Coherence effects have been used in the conversion of solar axions through Bragg diffraction with the electric field of a crystal [13, 22], but, as the enhancement relies on the solar axions being converted into X-rays, it is not compatible with axions produced by optical lasers considered here. Additionally, in our case the momentum transfer and the spatial structure along the direction of beam propagation are intrinsically linked since they are both given by the frequency of the light in the standing wave, precluding coherence along the whole laser beam without some kind of external temporal modulation.

Let us consider a probe photon beam interacting with a standing wave (Fig. 3). We approximate the probe beam photons as point-like, since the probe wavelength is much smaller than the standing wave wavelength. The structure factor associated with the momentum-transfer (\mathbf{q}) is then given by

$$I(\mathbf{q}) = \sum_{i,j=1}^{N_1} e^{i\mathbf{q} \cdot (\mathbf{x}_i - \mathbf{x}_j)}, \quad (8)$$

where \mathbf{x}_i are the positions of the standing wave photons in the interaction region. The momentum transfer q is simply the momentum $\pm k$ of a photon in beam 1 for our elastic scattering. Generically, the sum over these phases will be incoherent, and so only the diagonal piece of the matrix will contribute, leading to a scaling proportional to N_1 . To achieve some form of coherence, the off-diagonal pieces ought to constructively interfere, providing a quadratic scaling. We have

$$I(\mathbf{q}) = \left(\frac{2N_1}{L} \right)^2 \left| \int_{-\frac{L}{2}}^{\frac{L}{2}} dx \cos^2(kx + \phi) e^{-ikx} e^{-\frac{x^2}{2w^2}} \right|^2, \quad (9)$$

where L is the width of the probe beam and the Gaussian models the intensity fall-off of the standing wave, governed by its Rayleigh length w . The phase ϕ that the probe photon sees is dependent on where the probe beam falls on the standing wave. To achieve the largest coherence, we must achieve a focus such that $L \simeq \lambda_1/2$. For such a scenario, we have $w \gg L$, and we find that the structure factor is rather insensitive to ϕ , varying by a factor of 4 over its range.

Once created the axions must be reconverted into photons to be detected. Since the axions are on-shell, light, and weakly coupled, they propagate over a macroscopic

distance. Such a decay into a visible photon can in principle be enhanced by stimulated processes, similar to what has been proposed for QED precision tests with three colliding lasers [23]. An additional (third) beam is introduced into the interaction region and can induce a stimulated decay into a photon. However, given available photon numbers, stimulated decay is negligible for any interesting coupling constant [19]. Hence, we will adopt the usual approach of reconverting the axions in a magnetic field placed after an intervening wall.

As for any LSW experiment, the reconversion region is filled by a background magnetic field B over a length L . The mixing probability is given by [9, 24]

$$P_{a \rightarrow \gamma\gamma} = \frac{g_{a\gamma\gamma}^2 B^2 L^2}{\beta_a} \left(\frac{\sin qL/2}{qL} \right)^2, \quad (10)$$

with the momentum transfer $q = \sqrt{\omega_a^2 - m_a^2} - \omega_a$, the axion energy $\omega_a = \omega_1 + \omega_2$, and β_a the axion velocity. The sinc function describes the momentum modes present in the magnetic field, arising from taking the spatial Fourier transform of the magnetic field, assumed constant over the length L , and zero otherwise. Adler's photon splitting theorem, which would cause the diagram in Fig. 1 to vanish for $L \rightarrow \infty$ [25], is thus avoided as the magnetic field can transfer momentum.

The number of detected photons is finally given by

$$N_\gamma = \int \int I(q) N_2 P_{\gamma\gamma \rightarrow a} P_{a \rightarrow \gamma\gamma} f_1(\omega_1) f_2(\omega_2) d\omega_1 d\omega_2, \quad (11)$$

where we have assumed the laser beam frequency distribution is given by equation (4), and ω_1 and ω_2 are the standing wave and probe frequencies, respectively.

The proposed experiment is most sensitive to a hypothetical axion whose mass matches the central frequencies of the two beams, that is, $m_a = \sqrt{2\omega_1\omega_2(1 - \cos\theta_{12})}$, by 4-momentum conservation. Due to the non-zero bandwidth of the incoming laser beams, axions of different masses can be produced with decreasing probability moving away from the central frequencies of the beams. The width of the sensitivity region, which we define as the mass region within which the coupling bound varies by less than $\sqrt{2}$, for the case of two beams of similar spectral distribution, is

$$\frac{\delta m_a}{m_a} \simeq \frac{\Delta_1}{\omega_1} + \frac{\Delta_2}{\omega_2}. \quad (12)$$

Hence in order to scan across a range of possible axion masses, we must take shots in increments of angle δ_{12} given by

$$\delta_{12} \simeq 2 \frac{\delta m_a}{m_a} (\csc\theta_{12} - \cot\theta_{12}). \quad (13)$$

This angular step size and corresponding mass region is shown in Figure 4. Note that there is an upper bound on

the mass that can be probed. We require that the spread in momentum is small enough so that an axion will enter the finite aperture of the reconversion region. Assuming an aperture size of 0.1 rad, we must have $\theta_{12} \leq \theta_{\max}$, $\theta_{\max} \simeq \pi - 0.2$.

We now estimate the experimental feasibility of the proposed setup by calculating the expected number of photons produced. We will consider an idealised detector capable of detecting single photons. We will also assume that the detector is placed inside a shielded reconversion cavity, and that any noise photons can be easily rejected given that they will either lie outside the axion energy range, or are not coincident with the laser beam timing.

We see from equation 11 that to increase the signal we must maximise the laser intensity. Some of the current or near-commissioning high-power laser facilities can achieve numbers of up to $\sim 10^{21}$ photons per beam. The Aton 4 (10 PW) laser at ELI-beamlines, for example, can operate at a central optical frequency of 1.55 eV with spectral width of $\Delta = 0.05$ eV, and pulse length of $\tau = 100$ fs. We consider the scenario in which both beams are focused down to their respective wavelengths. Frequency doubling and tripling is also possible, as is the beam splitting in two independent arms. We consider the beams to be focused down to their respective photon wavelengths. Finally, we consider, in the reconversion region, a magnetic field of strength 10 T, although the limits on $g_{a\gamma\gamma}$ scale only as $B^{-1/2}$. We use these parameters to evaluate equation 11.

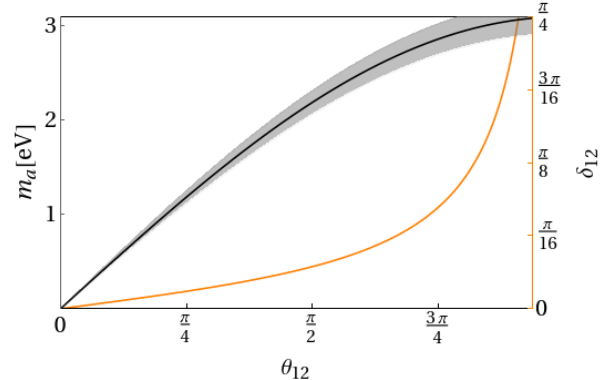


FIG. 4. The orange curve plots the angular step size δ_{12} against the chosen angle θ_{12} for each shot. Here the spectral width is $10/\tau$. On the left axis, the black curve indicates the central mass probed for a given θ_{12} and $\omega_1^0 = \omega_2^0 = 1.55$ eV, the shaded region indicates the width $\pm\delta m_a$. Assuming a minimum possible step-size $\delta_{12} \gtrsim 1^\circ$, the full mass range can be scanned in ~ 30 shots. This step size imposes a lower bound on $\theta_{12} \gtrsim 0.4$ rad corresponding to $m_a \gtrsim 0.6$ eV. Momentum spreading imposes an upper bound for these frequencies on $m_a \lesssim m_a(\theta_{\max}) = 2.47$ eV, as explained in the main body of the text.

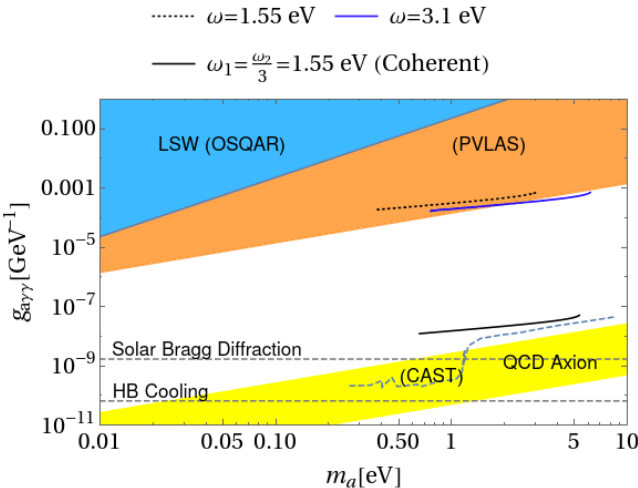


FIG. 5. Exclusion plot for axion parameter space. The light blue region shows existing bounds from the OSQAR experiment [26]; the orange region is excluded by PVLAS [16]; the dashed blue line depicts CAST constraints [11]; the lower horizontal dashed line comes from stellar cooling lifetimes [27] and the upper from solar Bragg diffraction experiments [13]. The dotted black and dark blue lines correspond to our proposal performed at $\omega = 1.55$ eV and the first harmonic, respectively, with ELI parameters and no substructure coherence. The black line shows the possible bounds using standing wave coherence. The region above the line is excluded in each case. The QCD axion region indicates particular theoretical predictions for where the axion might be, given dark matter abundances [28].

Figure 5 shows the axion exclusion limits we expect to achieve with the proposed experiment. We see that our technique is able to access regions of parameter space that are not already excluded by existing LSW experiments. The lines in Figure 5 must be interpreted as the upper bound on $g_{a\gamma\gamma}$ and, for given laser parameters, they are constructed by changing the scattering angle as discussed earlier so that we constrain an order of magnitude in m_a . The scalar exclusion plot gives very similar bounds. The two upper lines in Figure 5 are obtained without any coherent enhancement. While PVLAS provides slightly better bounds, however, as discussed above, these suffer from irreducible Standard Model background limitations. Our proposed searches, on the other hand, have no such background. When scattering from coherent laser substructures is implemented, our bounds on the axion-photon coupling are competitive with CAST in the $1 - 5$ eV mass range, and model independent. Astrophysical bounds, as is the case for all laboratory experiments in this mass range, provide more stringent bounds, again with the caveat that they are model dependent.

Considering the progress in laser technology over the past decades [29], it is not inconceivable that laser intensities would grow further over the coming years to allow new parameter space to be probed. Given the cubic

scaling with photon number for coherent scattering, these advances can achieve a significant improvement of the bounds presented here, and more so compared to other LSW experiment. The mass range can also be extended by using XFELs, for which a higher degree of frequency tuning is possible. This would allow for easier scanning of parameter space.

The experimental parameters we consider here do not maximise the coherence factor. In fact, the reconversion efficiency can be improved if the magnetic field were spatially varying, such that its Fourier transform components match the momentum transfer in the axion-photon transition. Moreover, the refractive index of the reconversion chamber could also be varied to reduce the difference in the axion mass and the effective photon mass, which would decrease the required momentum transfer. We have not yet included these effects in our analysis, and as such our results can be considered a lower bound on the performance of this technique at high-intensity laser facilities.

We would like to thank Prof Subir Sarkar, Rami Shelaya and especially Charlotte Palmer for many useful discussions. The research leading to these results has received funding from AWE plc. British Crown Copyright 2019/AWE.

* Authors to whom correspondence should be addressed: konstantin.beier@physics.ox.ac.uk

† giacomo.marocco@physics.ox.ac.uk

- [1] R. D. Peccei and Helen R. Quinn. CP conservation in the presence of pseudoparticles. *Phys. Rev. Lett.*, 38:1440–1443, Jun 1977.
- [2] R. D. Peccei and Helen R. Quinn. Constraints imposed by CP conservation in the presence of pseudoparticles. *Phys. Rev. D*, 16:1791–1797, Sep 1977.
- [3] Steven Weinberg. A New Light Boson? *Phys. Rev. Lett.*, 40:223–226, 1978.
- [4] Frank Wilczek. Problem of Strong P and T Invariance in the Presence of Instantons. *Phys. Rev. Lett.*, 40:279–282, 1978.
- [5] F. Miniati, Gérard Grégoire, B. Reville, and Subir Sarkar. Axion-driven cosmic magnetogenesis during the qcd crossover. *Physical Review Letters*, 121, 7 2018.
- [6] Edward Witten. Some Properties of $O(32)$ Superstrings. *Phys. Lett.*, 149B:351–356, 1984.
- [7] Asimina Arvanitaki, Savas Dimopoulos, Sergei Dubovsky, Nemanja Kaloper, and John March-Russell. String Axiverse. *Phys. Rev.*, D81:123530, 2010.
- [8] M. Tanabashi et al. Review of Particle Physics. *Phys. Rev.*, D98(3):030001, 2018.
- [9] P. Sikivie. Experimental Tests of the Invisible Axion. *Phys. Rev. Lett.*, 51:1415–1417, 1983. [,321(1983)].
- [10] Georg Raffelt and Leo Stodolsky. Mixing of the Photon with Low Mass Particles. *Phys. Rev.*, D37:1237, 1988.
- [11] V. Anastassopoulos, S. Aune, K. Barth, A. Belov, H. Bräuninger, Giovanni Cantatore, JM Carmona, JF Castel, SA Cetin, F. Christensen, et al. New cast limit on

- the axion–photon interaction. *Nature Physics*, 13(6):584, 2017.
- [12] H. Primakoff. Photoproduction of neutral mesons in nuclear electric fields and the mean life of the neutral meson. *Phys. Rev.*, 81:899, 1951.
- [13] R Bernabei, P Belli, R Cerulli, F Montecchia, F Nozzoli, A Incicchitti, D Prosperi, CJ Dai, HL He, HH Kuang, et al. Search for solar axions by primakoff effect in nai crystals. *Physics Letters B*, 515(1-2):6–12, 2001.
- [14] Joerg Jaeckel, Eduard Masso, Javier Redondo, Andreas Ringwald, and Fuminobu Takahashi. The Need for purely laboratory-based axion-like particle searches. *Phys. Rev.*, D75:013004, 2007.
- [15] R. Ballou, G. Deferne, M. Finger, M. Finger, L. Flekova, J. Hosek, S. Kunc, K. Macuchova, K. A. Meissner, P. Pugnat, M. Schott, A. Siemko, M. Slunecka, M. Sulc, C. Weinsheimer, and J. Zicha. New exclusion limits on scalar and pseudoscalar axionlike particles from light shining through a wall. *Phys. Rev. D*, 92:092002, Nov 2015.
- [16] Federico Della Valle, Aldo Ejlli, Ugo Gastaldi, Giuseppe Messineo, Edoardo Miliotti, Ruggero Pengo, Giuseppe Ruoso, and Guido Zavattini. The PVLAS experiment: measuring vacuum magnetic birefringence and dichroism with a birefringent FabryPerot cavity. *Eur. Phys. J.*, C76(1):24, 2016.
- [17] Stephen L. Adler. Photon splitting and photon dispersion in a strong magnetic field. *Annals Phys.*, 67:599–647, 1971. [,333(1971)].
- [18] Kirill Melnikov and Arkady Vainshtein. On dispersion relations and hadronic light-by-light scattering contribution to the muon anomalous magnetic moment. 2019.
- [19] Denis Bernard. On the potential of light by light scattering for invisible axion detection. *Nuovo Cim.*, A110:1339–1346, 1997. [,201(1997)].
- [20] Thomas Heinzl, Ben Liesfeld, Kay-Uwe Amthor, Heinrich Schwoerer, Roland Sauerbrey, and Andreas Wipf. On the observation of vacuum birefringence. *Opt. Commun.*, 267:318–321, 2006.
- [21] Peter J Martin, Bruce G Oldaker, Andrew H Miklich, and David E Pritchard. Bragg scattering of atoms from a standing light wave. *Physical review letters*, 60(6):515, 1988.
- [22] EA Paschos and Konstantin Zioutas. A proposal for solar axion detection via bragg scattering. *Physics Letters B*, 323(3-4):367–372, 1994.
- [23] E. Lundstrom, G. Brodin, J. Lundin, M. Marklund, R. Bingham, J. Collier, J. T. Mendonca, and P. Norreys. Using high-power lasers for detection of elastic photon-photon scattering. *Phys. Rev. Lett.*, 96:083602, 2006.
- [24] Stephen L. Adler, J. Gamboa, F. Mendez, and J. Lopez-Sarrion. Axions and ‘Light Shining Through a Wall’: A Detailed Theoretical Analysis. *Annals Phys.*, 323:2851–2872, 2008.
- [25] Stephen L Adler. Photon splitting and photon dispersion in a strong magnetic field. *Annals of Physics*, 67(2):599–647, 1971.
- [26] R. Ballou et al. New exclusion limits on scalar and pseudoscalar axionlike particles from light shining through a wall. *Phys. Rev.*, D92(9):092002, 2015.
- [27] Adrian Ayala, Inma Domínguez, Maurizio Giannotti, Alessandro Mirizzi, and Oscar Straniero. Revisiting the bound on axion-photon coupling from globular clusters. *Physical review letters*, 113(19):191302, 2014.
- [28] Luca Di Luzio, Federico Mescia, and Enrico Nardi. Redefining the axion window. *Physical review letters*, 118(3):031801, 2017.
- [29] Donna Strickland and Gerard Mourou. Compression of amplified chirped optical pulses. *Optics communications*, 55(6):447–449, 1985.